IEEE Access
Multidisciplinary | Rapid Review | Open Access Journal

Received May 20, 2019, accepted June 16, 2019, date of publication June 26, 2019, date of current version July 17, 2019.

Digital Object Identifier 10.1109/ACCESS.2019.2924577

Research on Wind Power Accommodation for an Electricity-Heat-Gas Integrated Microgrid System With Power-to-Gas

YUEWEN JIANG AND LIYUN GUO
College of Electrical Engineering and Automation, Fuzhou University, Fuzhou 350108, China
Fujian Smart Electrical Engineering Technology Research Center, Fuzhou 350108, China

Corresponding author: Yuewen Jiang (jiangyuewen2008@163.com)

This work was supported in part by the Natural Science Foundation of China under Grant 51707040, and in part by the Natural Science Foundation of Fujian Province in China under Grant 2018J01482.

ABSTRACT With the development of new energy on a large scale, the application of power-to-gas (P2G) technology provides novel ideas for the consumption of renewable energy such as wind power. This paper proposes a nonlinear optimal model of wind power accommodation for an electricity-heat-gas integrated microgrid with P2G, taking the minimum operating cost, the minimum wind curtailment, and the minimum comprehensive cost as objectives. On the basis of meeting the demand for electricity, heat and gas loads, the security constraints of the electricity microgrid, and the gas network are considered in connection with the operating characteristics of the P2G devices. The optimization software GAMS is used to solve this model. Finally, the integrated system of a 14-bus microgrid and a modified 20-bus gas network is adopted for demonstrating the effectiveness of the application of the P2G to improve wind power accommodation capability.

INDEX TERMS Microgrid, wind power accommodation, power to gas, electricity-heat-gas integrated energy.

I. INTRODUCTION

With the increasingly contradiction between the economic growth mode with high consumption and pollution and the global energy crisis and environmental issues, the transformation of energy structure and the improvement of energy utilization have become a strategic orientation of social development [1]. Renewable energy sources, in particular wind power, have the characteristics of sustainability and significant environmental benefits, so it has been massively invested and developed by countries all over the world. The integration of renewable energy into the microgrid system brings energy value and saves fuel cost. On the other hand, the volatility and intermittency of the output will affect the normal operation of the system. However, a microgrid system can integrate multiple energy sources and types of loads [2]. According to the characteristics of each energy source, the mutual coordination among multi energy carriers can reduce or eliminate the uncertainty of renewable energy, which is more conducive to the safe consumption of renewable energy.

Recently, wind power is the most promising power generation among renewable energy sources, and some literatures have been studying on the wind power accommodation in a microgrid system. Due to the fact that the inherent intermittency and variability of wind power complicates the operation in a microgrid, a stochastic problem of energy scheduling is formulated in [3]. Reference [4] put forward an optimal energy management strategy in an industrial microgrid with high-penetration renewables, and the objective includes minimization of fuel cost, operation and maintenance costs without the consideration of startup cost. In order to improve the wind power accommodation, reference [5] measures the wind power accommodation capability, and constructs a wind power integration assessment model to maximize the accommodation of wind power and the operating economy of the system. In [6], based on the existing power supply structure, the peak load regulation capacity of a power grid can be improved by allowing the abandonment of a certain marginal amount of electricity, thereby further improving the wind power accommodation. Reference [7] analyzes the changes of grid power flow and node voltage, and alters the user's electricity habits through the demand response, thus suppressing wind power fluctuation and anti-peak characteristics and improving the space to absorb wind power. In [8], the output of cogeneration units can be adjusted flexibly by configuring heat storage devices,

The associate editor coordinating the review of this manuscript and approving it for publication was Huiqing Wen.

so as to enhance the integrated ability of wind power in a microgrid.

Meanwhile, considering that the natural gas network with similar energy flow to the power grid has ideal energy storage and transportation advantages, the integrated electricity microgrid and natural gas network can generate new ideas for new energy consumption [9], [10]. Traditional grid and natural gas network are unilaterally coupled only through gas-fired units that convert natural gas into electrical energy, and the progress of P2G technology has made it possible to bi-directionally flow energy. In recent years, scholars have conducted relevant research on the important energy interconnection unit of P2G, and have made certain progress. References [11], [12] expound the development potential of P2G technology. Reference [13] analyzes the technical characteristics of P2G, and objectively evaluates its application prospects. In [14], P2G technology is regarded as an effective means to achieve long-term and wide-area energy storage, and its possible forms in the coordinated operation of electricity and gas are proposed. In the field of electricity-gas integrated energy research, reference [15] proposes a reliability assessment method for the energy-flow model of the electricity-gas integrated system. In [16], via a two-stage optimization, power system operation with P2G is analyzed to assess the gas production from otherwise curtailed renewables. However, there is lack of assessment of renewable energy efficiency. In [17], The interdependence between power grid and natural gas network is discussed, and a multi-objective framework which satisfies the network's security constraints is proposed for the coordinated operation in an integrated system. However, the interaction between the electricity and natural gas networks only originates from gas-fired generation units. In view of the characteristics of P2G devices, power grid and natural gas network, an operating strategy of electricity-gas multi-energy system is proposed in [18]. However, in [10] and [18], the integrated system does not include a heat system. As an autonomous system that can realize self-control, protection and management, a microgrid can not only have electricity and gas load, but also supply heat load with the waste heat of power plants, which is an effective way to realize the sustainable development of power industry through the cascade utilization of energy, promoting the utilization rate of comprehensive energy. In addition, the above existing research focuses on the pursuit of minimization of operating costs, ignoring the potential utilization of renewable energy.

In this case, the cogeneration microgrid with P2G devices, the natural gas network and heat network are coupled by considering the energy conversion, and the goal of this paper is to quantitatively evaluate the wind power accommodation from two aspects: operation cost and wind curtailment. Taking into account the power flow of the microgrid and the constraints of natural gas network and heat energy, a nonlinear optimization model of an electricity-heat-gas integrated microgrid with P2G devices is constructed with the objectives which are the minimum operating cost, the minimum wind curtailment and the minimum comprehensive cost, respectively.

Based on the above, the main contributions of this paper are twofold: i) schedule the dispatchable multi-energy suppliers in an electricity-heat-gas integrated microgrid system to enhance the wind power accommodation under different operating mode, and ii) analyze the operation of P2G devices in a an electricity-heat-gas integrated system with different wind power penetration and the influence of P2G devices on the increase of wind power integration.

The paper is structured as follows. Section II introduces the P2G technology. Section III describes the structure of an electricity-heat-gas integrated microgrid system, and establishes the corresponding wind power accommodation optimization model. Simulation results are shown in section IV and section V presents the conclusions.

II. OVERVIEW OF P2G TECHNOLOGY

As a potential energy storage method, P2G technology can convert electrical energy into fuel gas, and its process can be divided into power-to-hydrogen and power-to-natural gas according to the different products. In both, power-to-hydrogen is a process of electrolyzing water to form hydrogen and oxygen, namely $2H_2O \rightarrow 2H_2 + O_2$, and its energy conversion efficiency reaches 75%-85%. The power-to-natural gas is based on power-to-hydrogen, and the hydrogen generated by the electrolyzed water and carbon dioxide are further reacted under the action of the catalyst to generate water and methane, namely $CO_2 + 4H_2 \rightarrow CH_4 + 2H_2O$, and the energy conversion efficiency is 75%-80%. Hence, the comprehensive efficiency of power-to-natural gas is between 45% and 60%. Compared to power-to-natural gas, the energy dissipation of power-to-hydrogen is less, but there is a risk of hydrogen embrittlement and infiltration if the hydrogen is fed into natural gas pipelines [19]. Therefore, the P2G technology mentioned in this paper is power-to-natural gas.

The P2G device, as a unit connecting power grid and gas network, has two attributes: electricity load and natural gas source. Its energy conversion equation can be expressed as follows:

$$Q_i^{\mathrm{P2G}}(t) = \frac{P_i^{\mathrm{P2G}}(t)\eta_{\mathrm{P2G}}}{H_{\mathrm{G}}} \tag{1}$$

where $Q_i^{\mathrm{P2G}}(t)$ is the natural gas flow generated by the i-th P2G device in period t; $P_i^{\mathrm{P2G}}(t)$ is the active power consumed by the i-th P2G device in period t; η_{P2G} is the conversion efficiency of P2G devices; and H_{G} is the heating value of natural gas.

III. WIND POWER ACCOMMODATION OPTIMIZATION MODELING OF MICROGRID WITH P2G

A. STRUCTURE DESCRIPTION OF MICROGRID INTEGRATED SYSTEM

The P2G multi-source microgrid integrated system in this paper consists of micro turbines (MTs), fuel cells (FCs), diesel engines (DEs), wind turbines (WTs), waste heat boilers (WHs), gas boilers (GBs), P2G devices, heat storages (HSs), and electricity, heat and gas loads. The structure is shown in Fig. 1.

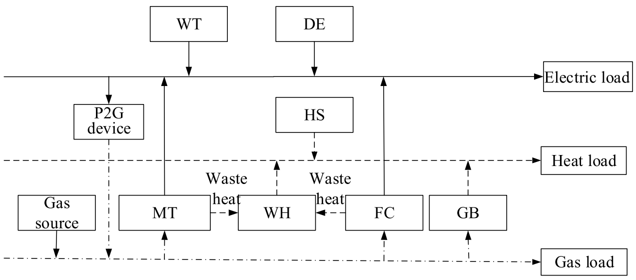

FIGURE 1. **Multi-source integrated microgrid with P2G.**

The MTs, FCs and GBs are fueled by natural gas, wherein MTs and FCs convert chemical energy into electrical energy, and GBs transform chemical energy into thermal energy. P2G devices are used as electric load in the power grid and as gas sources in the gas network; WHs supply heat to the system by recovering the waste heat generated by MTs and FCs; and HSs are charged and discharged according to the real-time heating condition of the system. In a word, the load supply of the whole system is as follows: the electricity load is supplied by MTs, FCs, WTs and DEs; the heat load is supplied by WHs, GBs and HSs; and the gas load is supplied by gas sources and P2G devices.

B. ESTABLISHMENT OF MICROGRID WIND POWER ACCOMMODATION OPTIMIZATION MODEL

Under different dispatching modes, the start-up and shutdown arrangements and energy supply plans of microgrid units are different, leading to different wind power accommodation. As a result, this paper takes the hourly output of energy suppliers in microgrid and natural gas network and the start-up and shutdown of distributed generation as decision variables, aiming at minimizing the operating cost, the wind curtailment and the comprehensive cost of the electricity-heat-gas microgrid system, respectively. Taking into account the balance of electricity, heat and natural gas flow, network constraints, and characteristics of each unit, a wind power accommodation optimization model for cogeneration microgrid with P2G devices is established.

Mode 1: the minimum operating cost of an electricity-heat-gas microgrid

The system operating cost, including equipment maintenance cost, unit start-up cost, spinning reserve cost, and the cost of natural gas, can be expressed as:

$$\min F_1 = \sum_{t=1}^{T} (C_{\mathrm{om}}(t) + C_{\mathrm{st}}(t) + C_{\mathrm{r}}(t) + C_{\mathrm{w}}(t)) \tag{2}$$

where

$$C_{\mathrm{om}}(t) = \sum_{i=1}^{I} k_{\mathrm{om}}^{i} P_i(t) \tag{3}$$

$$C_{\mathrm{st}}(t) = \sum_{i=1}^{I} \max\left\{0, U_i^{\mathrm{G}}(t) - U_i^{\mathrm{G}}(t-1)\right\} C_{\mathrm{st},i}^{\mathrm{U}} \tag{4}$$

$$C_{\mathrm{r}}(t) = a_{up} \sum_{i=1}^{I} R_{Gi}^{up}(t) + a_{down} \sum_{i=1}^{I} R_{Gi}^{down}(t) \tag{5}$$

$$C_{\mathrm{w}}(t) = \rho_{\mathrm{w}} \sum_{i=1}^{I} Q_i^{\mathrm{W}}(t) \tag{6}$$

where $C_{\mathrm{om}}(t)$, $C_{\mathrm{st}}(t)$, $C_{\mathrm{r}}(t)$ and $C_{\mathrm{w}}(t)$ are the maintenance cost of equipments, the start-up cost of units, the reserve cost, and the cost of natural gas in period t; $P_i(t)$ is the output of the i-th device; k_{om}^{i} is the unit operation and maintenance cost of the i-th equipment; $C_{\mathrm{st},i}^{\mathrm{U}}$ is the start-up cost of the i-th unit; $U_i^{\mathrm{G}}(t)$ is the start-up and shutdown state of the i-th unit in period t where the value of 0/1 indicates the shutdown state/start-up state; a_{up} and a_{down} are the coefficients of the reserve cost function; $R_{\mathrm{G}i}^{\mathrm{up}}(t)$ and $R_{\mathrm{G}i}^{\mathrm{down}}(t)$ are the positive and negative spinning reserve of the i-th unit in period t, respectively; ρ_w is the unit price of natural gas; and $Q_i^{\mathrm{W}}(t)$ is the supply amount of the i-th gas source in period t.

Mode 2: the minimum wind power curtailment in an electricity-heat-gas microgrid

Under this operation mode, ignoring the economy of system operation and pursuing the maximum of wind power accommodation, the objective can be expressed as

$$\min F_2 = \sum_{t=1}^{T} (P_w^{\mathrm{pre}}(t) - W_k(t)) \tag{7}$$

where $P_w^{\mathrm{pre}}(t)$ is the output of wind power; and $W_k(t)$ is the accommodated wind power in period t.

Mode 3: The minimum comprehensive cost of an electricity-heat-gas microgrid

The comprehensive cost is a scheduling model aiming at minimizing the sum cost of operation and wind power curtailment. By introducing coefficient λ, the two objectives of operation cost and wind power curtailment are united in a unit of \$/kWh. Therefore, λ can be understood as a wind curtailment penalty factor or wind curtailment cost. The objective function can be expressed as:

$$\min F_3 = F_1 + \lambda F_2 \tag{8}$$

C. CONSTRAINTS

1) Electricity balance constraint

$$P_i^{\mathrm{MT}}(t) + P_i^{\mathrm{FC}}(t) + W_i(t) + P_i^{\mathrm{DE}}(t) - P_i^{\mathrm{P2G}}(t) - P_i^{\mathrm{L}}(t) + \sum_{j \in i} P_{ji}(t) = 0 \tag{9}$$

where $P_i^{\mathrm{MT}}(t)$, $P_i^{\mathrm{FC}}(t)$, and $P_i^{\mathrm{DE}}(t)$ are the output of MTs, FCs, and DEs, respectively, at node i in period t; $W_i(t)$ is the wind power accommodation at node i in period t; $P_i^{\mathrm{P2G}}(t)$ is the active power consumed by P2G devices at node i in period t; $P_i^{\mathrm{L}}(t)$ is the electric load at node i in period t; $P_{ji}(t)$ is the power flow on the line from node j to node i in period t, and $j \in i$ indicates that node j is connected to node i.

2) Gas balance constraint

$$Q_i^{\mathrm{W}}(t)+Q_i^{\mathrm{P2G}}(t)-Q_i^{\mathrm{MT}}(t)-Q_i^{\mathrm{FC}}(t) -[Q_i^{\mathrm{CF}}(t)+Q_i^{\mathrm{F}}(t)]-Q_i^{\mathrm{L}}(t)+\sum_{j\in i}Q_{ji}^{\mathrm{gas}}(t)=0 \quad (10)$$

where $Q_i^{\mathrm{MT}}(t)$ and $Q_i^{\mathrm{FC}}(t)$ are the gas flow consumed by MTs and FCs, respectively, at node i in period t; $Q_i^{\mathrm{CF}}(t)$ and $Q_i^{\mathrm{F}}(t)$ are the gas flow through compressor connected to node i and the flow consumed by compressor, respectively, in period t; $Q_i^{\mathrm{L}}(t)$ is the gas load at node i in period t; and $Q_{ji}^{\mathrm{gas}}(t)$ is the flow of line from node j to node i in period t.

3) Heat balance constraint

$$H^{\mathrm{GB}}(t)+H^{\mathrm{WH}}(t)+H_{\mathrm{dis}}^{\mathrm{HS}}(t)-H_{\mathrm{ch}}^{\mathrm{HS}}(t)-H^{\mathrm{L}}(t)=0 \quad (11)$$

where $H^{\mathrm{GB}}(t)$ and $H^{\mathrm{WH}}(t)$ are the heat production of GBs and WHs, respectively, in period t; $H_{\mathrm{ch}}^{\mathrm{HS}}(t)$ and $H_{\mathrm{dis}}^{\mathrm{HS}}(t)$ are the charging and discharging heat of HSs, respectively, in period t; and $H^{\mathrm{L}}(t)$ is the heat load of period t.

4) Electricity network constraints

The active power supply constraint is

$$U_i^{\mathrm{G}}(t)P_{\mathrm{G}i\min}\le P_{\mathrm{G}i}(t)\le U_i^{\mathrm{G}}(t)P_{\mathrm{G}i\max} \quad (12)$$

The ramp rate constraint is

$$-R_{\mathrm{G}i}^{\mathrm{down}}\Delta T\le P_{\mathrm{G}i}(t)-P_{\mathrm{G}i}(t-1)\le R_{\mathrm{G}i}^{\mathrm{up}}\Delta T \quad (13)$$

The spinning reserve constraints are

$$R_{\mathrm{G}i}^{\mathrm{up}}(t)\le \min\left\{R_{\mathrm{G}i}^{\mathrm{U}}\Delta T, P_{\mathrm{G}i\max}-P_{\mathrm{G}i}(t)\right\} \quad (14)$$

$$R_{\mathrm{G}i}^{\mathrm{down}}(t)\le \min\left\{R_{\mathrm{G}i}^{\mathrm{D}}\Delta T, P_{\mathrm{G}i}(t)-P_{\mathrm{G}i\min}\right\} \quad (15)$$

$$\sum_{i=1}^{I}R_{\mathrm{G}i}^{\mathrm{up}}(t)\ge\sigma\sum_{k=1}^{K}W_k(t) \quad (16)$$

$$\sum_{i=1}^{I}R_{\mathrm{G}i}^{\mathrm{down}}(t)\ge\sigma\sum_{k=1}^{K}W_k(t) \quad (17)$$

where $P_{Gi\max}$ and $P_{Gi\min}$ are the maximum and minimum power generation of unit i, respectively; $R_{\mathrm{G}i}^{\mathrm{up}}$ and $R_{\mathrm{G}i}^{\mathrm{down}}$ are the ramp-up and ramp-down rates of unit i, respectively; and σ is the prediction error of wind power output.

The wind power output constraint is

$$0\le W_k(t)\le P_w^{\mathrm{pre}}(t) \quad (18)$$

$$P_w^{\mathrm{Pre}}=P_w^{\mathrm{fore}}+\varepsilon_w \quad (19)$$

where $P_w^{\mathrm{fore}}(t)$ is the output prediction of wind power. In this paper, the wind power prediction error is simulated in the form of a normal distribution. The mean value of the given distribution is 0, and the magnitude of the error level is expressed by the magnitude of standard deviation. This distribution can be expressed as

$$\varepsilon\sim\left(\mu,\sigma^2\right) \quad (20)$$

where ε_w is the wind power prediction error.

The voltage constraint is

$$U_{i\min}\le U_i(t)\le U_{i\max} \quad (21)$$

Line power flow constraints are

$$P_l^{\min}\le P_{ij}(t)\le P_l^{\max} \quad (22)$$

where $P_l^{\min}$ and $P_l^{\max}$ are the lower and upper power flow limits of the line l, respectively.

5) Gas network Constraints

The gas flow of pipelines constraint is

$$Q_{ij}^{\mathrm{gas}}(t)=K_{ij}S_{ij}(t)\sqrt{S_{ij}(t)\left[(p_i^{gas}(t))^2-(p_j^{gas}(t))^2\right]} \quad (23)$$

$$S_{ij}(t)=\begin{cases}+1 & p_i^{gas}(t)\ge p_j^{gas}(t)\\ -1 & \text{others}\end{cases} \quad (24)$$

where K_{ij} is a constant related to the pipeline temperature, length, inner diameter, natural gas compression factor, etc; $S_{ij}(t)$ is the direction of pipeline gas flow in period t, positive from node i to node j; $p_i^{gas}(t)$ and $p_j^{gas}(t)$ represent upstream and downstream pressure of pipeline from node i to node j, respectively.

Compressor flow constraints are

$$P_i^{\mathrm{com}}(t)=B_kQ_i^{\mathrm{CF}}(t)[(\frac{\pi_n(t)}{\pi_m(t)})^{Z_k}-1] \quad (25)$$

$$Q_i^F(t)=\alpha_k+\beta_kP_i^{com}(t)+\gamma_k[P_i^{com}(t)]^2 \quad (26)$$

where B_k and Z_k are the characteristic coefficients of the compressor; $\pi_m(t)$ and $\pi_n(t)$ are the pressure at the inlet and outlet of the compressor, respectively, $P_i^{\mathrm{com}}(t)$ is the power consumed by the compressor; and α_k, β_k, and γ_k are the energy consumption coefficients.

The upper and lower limit constraint of gas resources is

$$Q_{\min,i}^W\le Q_i^W(t)\le Q_{\max,i}^W \quad (27)$$

where $Q_{\min,i}^W$ and $Q_{\max,i}^W$ are the lower and upper limits of the flow rate of gas source i, respectively.

Joint pressure constraint is

$$p_{\min,i}^{\mathrm{gas}}\le p_i^{\mathrm{gas}}(t)\le p_{\max,i}^{\mathrm{gas}} \quad (28)$$

where $p_{\min,i}^{\mathrm{gas}}$ and $p_{\max,i}^{\mathrm{gas}}$ are the lower and upper limits of pressure of node i, respectively.

6) Heat energy storage constraints are

$$0\le H_{\mathrm{ch}}^{HS}(t)\le\gamma_{\mathrm{ch}}C_{\mathrm{HS}} \quad (29)$$

$$0\le H_{\mathrm{dis}}^{HS}(t)\le\gamma_{\mathrm{dis}}C_{\mathrm{HS}} \quad (30)$$

$$E_{\mathrm{HS}\min}\le E_{\mathrm{HS}}(t)\le E_{\mathrm{HS}\max} \quad (31)$$

$$E_{\mathrm{HS}}(t)=(1-\tau)E_{\mathrm{HS}}(t-1)+[H_{\mathrm{ch}}^{HS}(t)\eta_{\mathrm{ch}}-\frac{H_{\mathrm{dis}}^{HS}(t)}{\eta_{\mathrm{dis}}}]\Delta t \quad (32)$$

where $E_{\mathrm{HS}}(t)$ is the heat storage capacity of period t; τ is the heat storage dissipation rate; η_{ch} and η_{dis} are the charging and discharging efficiencies of HS, respectively, in period t;

$\gamma_{\rm ch}$ and $\gamma_{\rm dis}$ are the maximum charging and discharging ratios of HS, respectively; and $C_{\rm HS}$ is the heat storage capacity.

7) Coupled element constraints

The power-to-gas coupling constraint is as (1).

Gas equipment coupling constraints are

$$P_i^{\rm MT}(t) = \eta_{\rm MT} Q_i^{\rm MT}(t) H_{\rm G} \tag{33}$$

$$P_i^{\rm FC}(t) = \eta_{\rm FC} Q_i^{\rm FC}(t) H_{\rm G} \tag{34}$$

$$H_i^{\rm WH}(t) = \eta_{\rm WH}(\gamma_{\rm MT} P^{\rm MT}(t) + \gamma_{\rm FC} P^{\rm FC}(t)) \tag{35}$$

$$H_i^{\rm GB}(t) = \eta_{\rm GB} Q_i^{\rm GB}(t) H_{\rm G} \tag{36}$$

where $\eta_{\rm MT}$, $\eta_{\rm FC}$, $\eta_{\rm WH}$, and $\eta_{\rm GB}$ are conversion efficiencies of MTs, FCs, WHs, and GBs, respectively; and $\gamma_{\rm MT}$ and $\gamma_{\rm FC}$ are heat-to-power ratios of MTs and FCs, respectively.

D. MODEL SOLVING

1) NONLINEAR EQUIVALENCE OF MODEL

In view of the fact that the non-smoothness of the variable S_{ij} in the gas flow direction in the pipeline will cause computing problems, Eqn. (22) is altered by introducing auxiliary 0-1 variables u_{ij}^s and u_{ji}^s. When the actual gas flow direction is $i \rightarrow j$, $u_{ij}^s = 1$ and $u_{ji}^s = 0$. On the contrary, when the actual gas flow direction is $j \rightarrow i$, $u_{ij}^s = 0$, $u_{ji}^s = 1$. Eqn. (22) can be equivalent to:

$$u_{ij}^s + u_{ji}^s \leq 1 \tag{37}$$

$$S_{ij} = u_{ij}^s - u_{ji}^s \tag{38}$$

$$(Q_{ij}^{gas})^2 = K_{ij}^2 S_{ij}((p_i^{gas})^2 - (p_j^{gas})^2) \tag{39}$$

$$-u_{ji}^s Q_{ij}^{\max} \leq Q_{ij}^{gas} \leq u_{ij}^s Q_{ij}^{\max} \tag{40}$$

2) SOLUTION TOOL

General Algebraic Modeling System (GAMS) is a commercial software for optimal numerical analysis, whose prominent feature is that the model is allowed to be independent of the solution algorithm. It can solve various optimization problems such as linear programming, non-linear programming, mixed integer non-linear programming, etc. by calling appropriate solvers and is widely used in scientific research and engineering practice [20]. The optimization model of the electricity-heat-gas integrated microgrid system with P2G devices in this paper is a mixed integer non-linear optimization problem.. Therefore, the optimization software GAMS is used to solve the problem.

IV. CASE STUDY

A. CASE DESCRIPTION

This paper takes a 14-node microgrid system connected to a modified 20-node natural gas network as an example. The structure diagram of the electricity-heat-gas microgrid is shown in Fig. 7. The specific parameters of the microgrid are described in [21]. The parameters of the pipelines, compressor and pressure limit of each node are shown in [22]. The MTs are connected to nodes 3 and 11; the FCs and DEs are respectively connected to nodes 6 and 12; and the WTs are at node 7. In the microgrid area, the MTs at nodes 3 and 6 are connected to the gas network nodes 3 and 12, respectively; the FCs at node 11 are connected to the gas network node 16; and the P2G devices at node 7 are connected to node 5 of the gas network. W1, W2, and W3 are three different gas sources, with the upper limit of 60m^3/h of gas supply. Assume that the capacity of the WTs is large enough. The parameters of energy conversion devices and the HSs are shown in Tabs. 4 and 5, respectively. Take one day as a cycle, divide the whole day into 24 time periods. Fig. 2 shows the predicted load curve throughout the day. The wind power forecast output is shown in Fig. 8. The standard deviation of wind power output prediction error is set to 10% of wind power forecast output. The price of natural gas is 0.45\$/m^3.

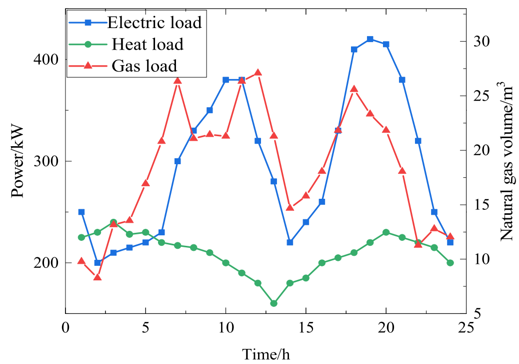

FIGURE 2. Different kinds of load forecast.

B. OPERATION RESULTS AND ANALYSIS

The optimization results under the three scheduling modes of the minimum operating cost (Obj. 1), the minimum wind power curtailment (Obj. 2), and the minimum comprehensive cost (Obj. 3) are shown in Tab. 1. It can be seen that the system operation cost is the lowest while there is a large amount of wind curtailment based on Obj. 1. When Obj. 2 is optimized, the wind power accommodation is larger, but the operation cost is also at a higher level. In terms of Obj. 3, the system operating cost and the wind curtailment are traded off. That is to say, the amount of wind curtailment is reduced by sacrificing certain economy, so as to improve the system's wind power accommodation. In Model 3, the value of λ is taken as 0.02\$/kWh.

TABLE 1. Optimization results under different scheduling modes.

Scheduling mode	F_1/\$	F_2/kWh
Mode 1	-716	-3413
Mode 2	1068	0
Mode 3	749	767

Considering the different importance degree of wind curtailment, this paper takes the wind curtailment penalty factor as 0.01\$/kWh, 0.02\$/kWh and 0.03\$/kWh respectively to optimize the model, and the results are shown in Tab. 2. As can be observed, with the increase of wind curtailment

TABLE 2. Comprehensive optimization results for different values of λ.

λ/($·kWh)	F_1/$	F_2/kWh
0.01	-708	3430
0.02	749	1767
0.03	770	59

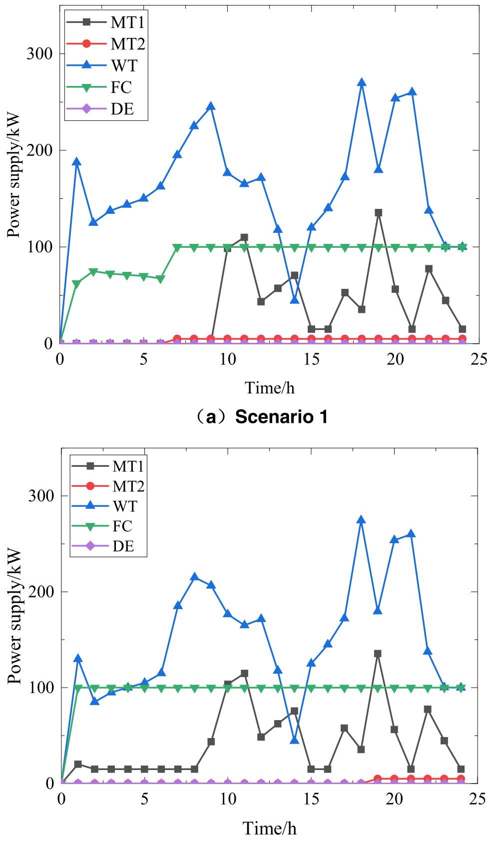

(a) Scenario 1

(b) Scenario 2

FIGURE 3. Electricity supply of micro-sources.

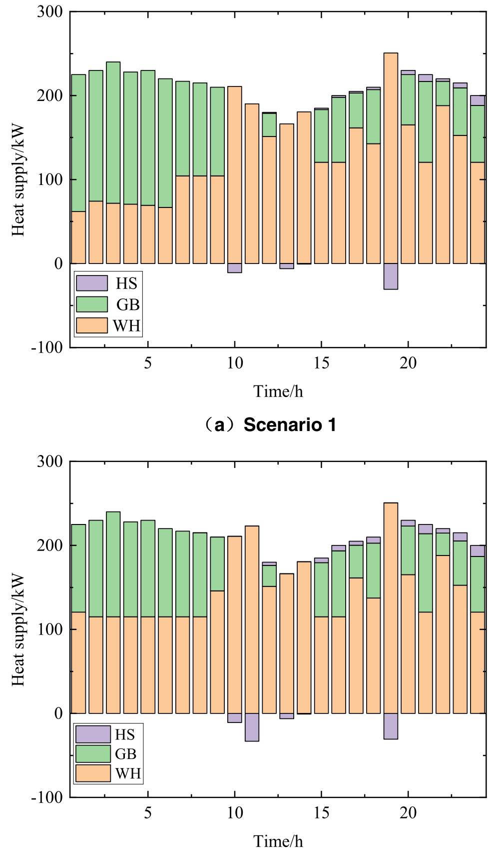

(a) Scenario 1

(b) Scenario 2

FIGURE 4. Heat supply of micro-sources.

penalty factor λ, wind curtailment decreases. In order to accept wind power to a greater extent the frequency of start-up and shutdown of units increases, resulting in a growing operating cost. At the same time, more spinning reserve is required, which also increases the operating cost.

In order to analyze the impact of the P2G devices on the wind power accommodation of the microgrid, the following two scenarios are set up in this paper. Scenario 1 considers the one-way coupling operation of the microgrid and natural gas network, that is, P2G devices are not considered, and the microgrid and natural gas network are only coupled by gas-fired units (including MTs, FCs and GBs); Scenario 2 considers the two-way coupling operation of microgrid and natural gas network, that is, the microgrid and natural gas network form a closed loop through gas-fired units and P2G devices. In both scenarios, the value of λ is taken as 0.03$/kWh.

Using model 3 to deal with the two scenarios respectively, the electricity supply of each micro-source is illustrated in Fig. 3 and the heat supply is demonstrated in Fig. 4. Generally speaking, compared to other electricity sources, the WTs have more electricity supply in the whole dispatching cycle, which indicates that a microgrid is a reliable carrier to absorb renewable energy. Meanwhile, due to the more electric load and less heat load during the period from 10:00 to 12:00, the surplus heat generated by the WHs can be stored by the HSs, that is, the negative value part in Fig. 4. And the heat can be released during the period of 16:00 to 18:00 and 24:00 when the demand of electricity is not high but a certain heat demand, so as to make cogeneration system, consisting of the MTs, FCs and WHs, avoid working in a state of electricity based on heat amount.

Comparing the electricity and heat supply conditions of the two scenarios, we can discover that in scenario 1, there is no other ways to consume wind power except supplying electric load with other units, which limits the integration of wind power. In scenario 2, P2G devices are introduced, which can convert a portion of wind power into natural gas used in the gas network during the low electricity demand periods, facilitating wind power accommodation in the microgrid.

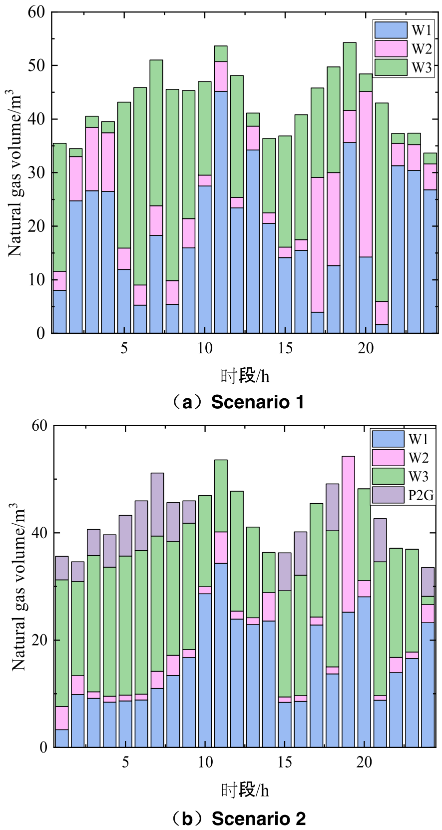

FIGURE 5. Natural gas supply.

The supply of natural gas in the natural gas network is shown in Fig. 5. The gas load in scenario 1 (including the fuel consumption of MTs, FCs, etc.) is completely supplied by the gas sources (W1, W2 and W3) where W1 and W3 play an important role during most periods. In Scenario 2, the output of each gas source has changed significantly after adding P2G devices, indicating that P2G devices change the energy distribution of the original gas network. Furthermore, in addition to the gas supply from P2G devices, the total gas supply of three gas sources is 1034.56 m^3 for Scenario 1 and 935.48 m^3 for Scenario 2. The total supply of gas sources is less for Scenario 2 than that for Scenario 1, because the generation cost of WTs is lower compared to conventional generators, leading to the cost of converting this energy from WTs into natural gas by P2G devices is also low. Therefore, P2G has the priority to supply gas, which reduces the gas supply ratio of three gas sources and the operating cost of the integrated system.

Fig. 6 illustrates the wind power accommodation in the microgrid with or without P2G devices. In the scenario without P2G devices, wind power cannot be completely consumed due to the mismatch of load and wind power output in time and other constraints of micro-generators. However, the addition of P2G devices can transfer the energy flow from the power grid to the gas network increasing wind power integration of 980.11 kW, and reducing the overall cost from \$773 to \$765 compared to the scenario without P2G devices.

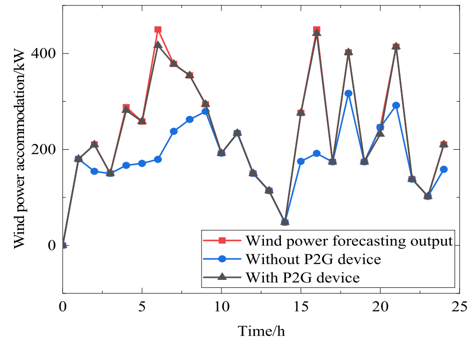

FIGURE 6. Wind power accommodation level of microgrid with or without P2G.

TABLE 3. The conversion energy of P2G devices under different wind power penetration levels.

wind power penetration/%	conversion energy of P2G devices/kWh	Wind energy accommodation/kWh
10%	262	5723
50%	478	2788
80%	1334	4959

Table 3 shows the conversion of P2G devices under different wind power penetration. We can see that when the penetration of wind power is low, the output of wind power is mostly accommodated by the microgrid, and the conversion power of P2G devices is less. With the increase of wind power penetration, the power converted through P2G devices increases.

V. CONCLUSION

Through the electricity-heat-gas integrated microgrid system with P2G devices, wind power accommodation optimization is modeled and analyzed on the basis of meeting different types of load demand. The conclusions are as follows:

1) Different dispatching modes lead to different optimization results of wind power accommodation in a microgrid. Only considering the economy of the system will worsen the wind curtailment (the wind curtailment is 3413kWh, but the operating cost is \$716), and only reckoning the minimization of the wind curtailment will deteriorate the operating cost (the wind curtailment is 0 kWh, but the operating cost is \$1068). Therefore, it is reasonable to evaluate the wind power accommodation with the objective of the minimum comprehensive cost, where the curtailment penalty factor need be set appropriately.
2) When wind power is surplus and electricity demand is low, P2G devices convert surplus wind power into natural gas for storage and use in the gas network, which enhances the wind power accommodation by 980.11kWh in a day.
3) Because the generation cost of WTs is lower compared to conventional generators, the cost of converting this energy from WTs into natural gas by P2G devices is also low so that P2G has the priority to supply gas,

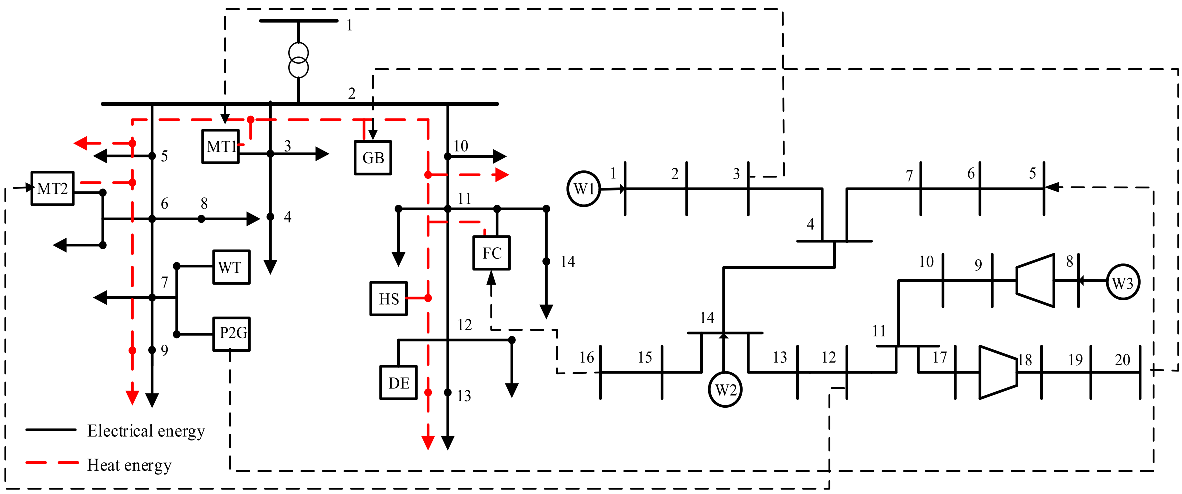

FIGURE 7. Structure of the electricity-heat-gas microgrid.

TABLE 4. Parameters of micro-sources.

	MT1	MT2	FC	DE	WH	GB	P2G
Lower limit/kW	15	5	10	10	0	0	0
Upper limit/kW	150	65	100	100	300	200	300
Ramping rate/ ($kW\cdot min^{-1}$)	5	5	2	5	-	-	-
Startup cost/$	0.47	0.15	0.42	0.1	-	-	-
Maintenance cost/($\$\cdot kWh^{-1}$)	0.016	0.016	0.03	0.01	0.01	0.01	0.01
Heat-to-power ratio	1.2	1.2	1.1	-	-	-	-

TABLE 5. Parameters of heat energy storage.

	C_{HS}/kW	η_{ch}	η_{dis}	γ_{ch}	γ_{dis}	τ	k_{om}/$
HS	100	0.95	0.95	0.4	0.4	0.01	0.01

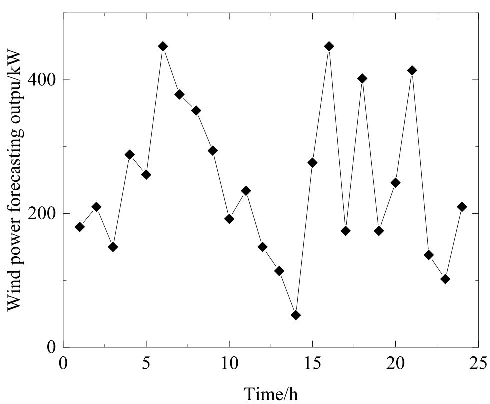

FIGURE 8. Output forecast of wind power.

which leads to the gas from gas sources reduces by 99.08 m^3, saving the operating cost of the integrated system.

The demand response will be further studied to optimize the operating cost and wind power accommodation in the future.

APPENDIX

See Tables 4 and 5, Figures 7 and 8.

REFERENCES

[1] B. Jiang, Z. Sun, and M. Liu, "China's energy development strategy under the low-carbon economy," *Energy*, vol. 35, no. 11, pp. 4257–4264, Nov. 2010.

[2] Z. Luo, W. Gu, Z. Wu, Z. Wang, and Y. Tang, "A robust optimization method for energy management of CCHP microgrid," *J. Mod. Power Syst. Clean Energy*, vol. 6, no. 1, pp. 132–144, Jan. 2018.

[3] W. Su, J. Wang, and J. Roh, "Stochastic energy scheduling in microgrids with intermittent renewable energy resources," *IEEE Trans. Smart Grid*, vol. 5, no. 4, pp. 1876–1883, Jul. 2014.

[4] H. Li, A. T. Eseye, J. H. Zhang, and D. H. Zheng, "Optimal energy management for industrial microgrids with high-penetration renewables," *Protection Control Mod. Power Syst.*, vol. 2, no. 1, p. 12, Dec. 2017.

[5] R. Prescott and G. C. Van Kooten, "Economic costs of managing of an electricity grid with increasing wind power penetration," *Climate Policy*, vol. 9, no. 2, pp. 155–168, Jan. 2009.

[6] C. Sun, Z. Bie, M. Xie, and J. Jiang, "Assessing wind curtailment under different wind capacity considering the possibilistic uncertainty of wind resources," *Electr. Power Syst. Res.*, vol. 132, pp. 39–46, Mar. 2016.

[7] T. Broeer, J. Fuller, F. Tuffner, D. Chassin, and N. Djilali, "Modeling framework and validation of a smart grid and demand response system for wind power integration," *Appl. Energy*, vol. 113, pp. 199–207, Jan. 2014.

[8] X. Wang and H. Li, "Multi-objectives combined electric heating dispatch model of wind power accommodation with heat storage device," *IET J. Mag.*, vol. 2017, no. 13, pp. 1539–1545, Nov. 2017.

[9] M. Ban, J. Yu, M. Shahidehpour, and Y. Yao, "Integration of power-to-hydrogen in day-ahead security-constrained unit commitment with high wind penetration," *J. Mod. Power Syst. Clean Energy*, vol. 5, no. 3, pp. 337–349, Apr. 2017.

[10] S. Clegg and P. Mancarella, "Integrated modeling and assessment of the operational impact of power-to-gas (P2G) on electrical and gas transmission networks," *IEEE Trans. Sustain. Energy*, vol. 6, no. 4, pp. 1234–1244, Oct. 2015.

[11] L. Schneider and E. Kötter, "The geographic potential of Power-to-Gas in a German model region—Trier-Amprion 5," *J. Energy Storage*, vol. 1, no. 1, pp. 1–6, Jun. 2015.

[12] C. Baumann, R. Schuster, and A. Moser, "Economic potential of power-to-gas energy storages," in *Proc. 10th Int. Conf. Eur. Energy Market (EEM)*, Stockholm, Sweden, May 2013, pp. 1–6.
[13] C. Breyer, E. Tsupari, V. Tikka, and P. Vainikka, "Power-to-gas as an emerging profitable business through creating an integrated value chain," *Energy Procedia*, vol. 73, pp. 182–189, Jun. 2015.
[14] M. Götz, J. Lefebvre, F. Mörs, A. M. Koch, F. Graf, S. Bajohr, R. Reimertn, and T. Kolb, "Renewable power-to-gas: A technological and economic review," *Renew. Energy*, vol. 85, pp. 1371–1390, Jan. 2016.
[15] Q. Zeng, J. Fang, J. Li, and Z. Chen, "Steady-state analysis of the integrated natural gas and electric power system with bi-directional energy conversion," *Appl. Energy*, vol. 184, pp. 1483–1492, Dec. 2016.
[16] S. Clegg and P. Mancarella, "Storing renewables in the gas network: Modelling of power-to-gas seasonal storage flexibility in low-carbon power systems," *IET Gener. Transmiss. Distrib.*, vol. 10, no. 3, pp. 566–575, Mar. 2016.
[17] I. G. Sardou, M. E. Khodayar, and M. T. Ameli, "Coordinated operation of natural gas and electricity networks with microgrid aggregators," *IEEE Trans. Smart Grid*, vol. 9, no. 1, pp. 199–210, Jan. 2018.
[18] G. Li, R. Zhang, T. Jiang, H. Chen, L. Bai, and X. Li, "Security-constrained bi-level economic dispatch model for integrated natural gas and electricity systems considering wind power and power-to-gas process," *Appl. Energy*, vol. 194, pp. 696–704, May 2017.
[19] D. Haeseldonckx and W. D'haeseleer, "The use of the natural-gas pipeline infrastructure for hydrogen transport in a changing market structure," *Int. J. Hydrogen Energy*, vol. 32, nos. 10–11, pp. 1381–1386, Jul./Aug. 2007.
[20] A. Brook, D. Kendrick, and A. Meeraus, "GAMS, a user's guide," *ACM Signum Newslett.*, vol. 23, nos. 3–4, pp. 10–11, Dec. 1988.
[21] A. K. Basu, A. Bhattacharya, S. Chowdhury, and S. P. Chowdhury, "Planned scheduling for economic power sharing in a CHP-based microgrid," *IEEE Trans. Power Syst.*, vol. 27, no. 1, pp. 30–38, Feb. 2012.
[22] J. Munoz, N. Jimenez-Redondo, J. Perez-Ruiz, and J. Barquin, "Natural gas network modeling for power systems reliability studies," in *Proc. IEEE Bologna Power Tech Conf.*, Bologna, Italy, Jun. 2004, p. 8.

YUEWEN JIANG received the Ph.D. degree from the College of Electrical Engineering and Automation, Fuzhou University, China, in 2009. In 2016, she was a Guest Researcher with the Department of Electrical Engineering, Technical University of Denmark, for one year. She is currently a Professor with Fuzhou University. Her current research interests include electricity market, renewable energy, and the optimization operation of power systems.

LIYUN GUO received the B.S. degree in electrical engineering and automation from Fuzhou University, Fujian, China, in 2016. She is currently pursuing the M.S. degree in power system and its automation with Fuzhou University. Her current research interests include the optimization operation of power systems and wind power grid-connected operation.